3.1 Introduction

Pyrochlore oxides being geometrically frustrated magnetic materials have attracted intense research attention due to its geometrical spin frustration driven novel ground states [1-3]. This plethora of interesting ground states is picked up by proper balance between exchange interaction, dipolar interaction and strong crystal field effect (CF). These special low temperature states include a fluid like states of spins, called spin liquid [4-6], spin glass,[7-9] spin ice [2,3,10-12], and order by disorder [13,14,15] etc. In pyrochlore $R_2Ti_2O_7$, the rare earth ions R^{3+}, occupying lattice points of corner shared tetrahedral play the main role in deciding the magnetic properties of the system. The R and Ti ions are individually occupying the lattice points of corner shared tetrahedra which collectively form inter-penetrating network of these tetrahedra, leading to frustration of their antiferromagnetic interactions. The unit cell of such structure contains 8 oxygen ions surrounding each R^{3+} ion inside a trigonally distorted cube, two of these are situated in diametrically opposite to each other along the <111> axis (D_{3D}) and other six are lying on the equatorial plane of the cube [16]. The R^{3+} ions are located at the vertices of two diametrically opposed tetrahedra of R^{3+} ions i.e they are all having six nearest neighbours [16]. Strong crystal field interaction with the D_{3D} symmetry causes the R^{3+} ionic magnetic susceptibility to be different along the D_{3D} axis and perpendicular to it, giving rise to Single ion anisotropy (SIA) [17]. In spin ice compounds ($Dy_2Ti_2O_7$ and $Ho_2Ti_2O_7$etc.), an unusual ground state is achieved by spins which is explained by Pauling's ice rule [10,18,19]. In spin ice materials, the f – electron spins of the rare earth ions R^{3+} (R=Dy, Ho) are large and hence treated classically and the CF driven Single ion anisotropy (SIA) renders the spins to be Ising like along the <111> axes [18,19]. Under this condition, the system does not become ordered by minimizing the dipolar interactions alone, thus end up with a frozen, non-collinear and disordered state at very low temperature $T<T_{ice}$ ~ 4K [10,19]. But for $Dy_2Ti_2O_7$, an additional unexpected peak in ac

susceptibility at~ 16K is found, which is absent in spin ice $Ho_2Ti_2O_7$ suggesting a strange difference between these compounds [10,12]. This spin freezing at T=16K >T_{ice} is attributed to the single spin freezing process [12,19-23]. The ice freezing (<4K) and this 16K single ion freezing are inter-linked by quantum tunnelling process (which is characterized by a very weak temperature dependence of spin relaxation times thus showing a plateau region below 12K) through the CF barrier and this is explained by creation and propagation of monopoles [19,24].

In this chapter, we have thoroughly investigated the temperature variation of magnetization, especially the ac susceptibility data of pyrochlore $Eu_2Ti_2O_7$ (ETO). The special $4f^6$ configuration of Eu^{3+} ion in ETO plays the key role in determining its electronic and magnetic properties. In the unit cell of ETO, each Eu^{3+} ion is surrounded by 8 oxygen atoms which form a trigonally distorted cube having a three-fold inversion D_{3D} symmetry. The interactions between the Eu^{3+} ions and surrounding 8 oxygen ions produce a crystal field with D_{3D} symmetry [25]. The strong spin-orbit coupling in Eu^{3+} ions results in forming its electronic pattern consisting of non-magnetic ground state $^7F_0$ and the first excited magnetic state $^7F_1$which lies closely above it. This first magnetic term $^7F_1$ is followed by other excited magnetic levels $^7F_{2\text{-}6}$ lying above $^7F_1$ successively. Again crystal field (CF) level splits into further levels e.g$^7F_1$ splits into a singlet and a doublet [25]. Thus, instead of having non-magnetic ground state, Eu^{3+} shows appreciable magnetic susceptibility. In previous reports on $Eu_2Ti_2O_7$, CF calculations showed planar single ion anisotropy (SIA) parallel to local<111> axes [25]. The SIA along with exchange and dipolar interactions was seen to produce exotic magnetic properties. However, a comprehensive study reporting its detailed ac susceptibility properties is hitherto unreported and thus, it provoked us to investigate its spin dynamics by ac susceptibility studies.

3.2 Experimental

The sample of $Eu_2Ti_2O_7$ was prepared by solid state reaction route. The flow chart of its preparation steps is shown in below:

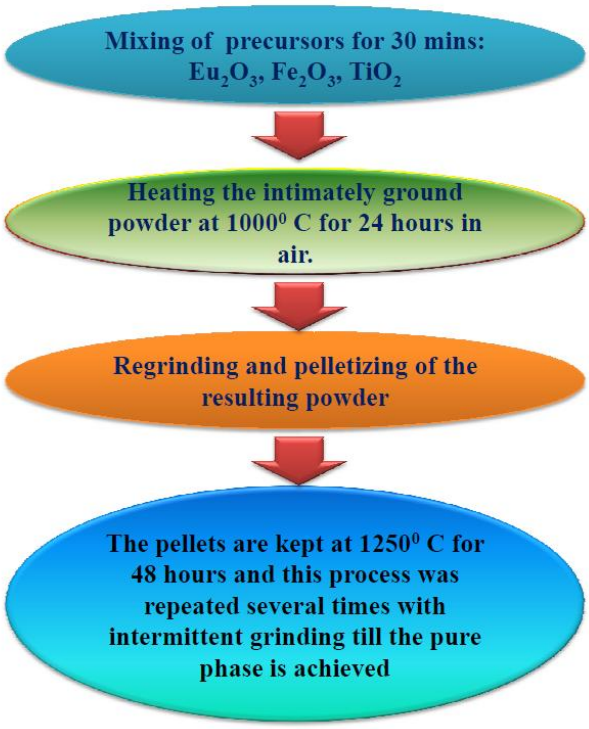

Figure. 3.1: *Flow chart of the sample preparation method.*

High purity (>99.99%) Eu_2O_3, Y_2O_3 and TiO_2 were mixed in stoichiometric ratio and ground for 0.5 hr, then heated in air at 1000^0 C for 24 hours. The resulting powder was reground and pressed into pellets and heated in air at 1250^0 C for 48 hours and the process was repeated several times. X-ray diffraction measurement was performed using Rigaku Miniflex II X-ray diffractometer. Fig. 3.2 shows the X-ray diffraction (XRD) data collected at room temperature (300K) along with its Rietveld refinement for pure $Eu_2Ti_2O_7$ sample. The XRD pattern was refined with space group $Fd\bar{3}m$. The position of Eu, Ti, O1 and O2 are 16d, 16c, 48f, 8c respectively. It suggests the samples are of good quality and confirms absence of chemically impure phase. We have performed ac and dc magnetic measurements using a Quantum Design magnetic property measurement system (MPMS) super conducting quantum interference devices (SQUID) magnetometer.

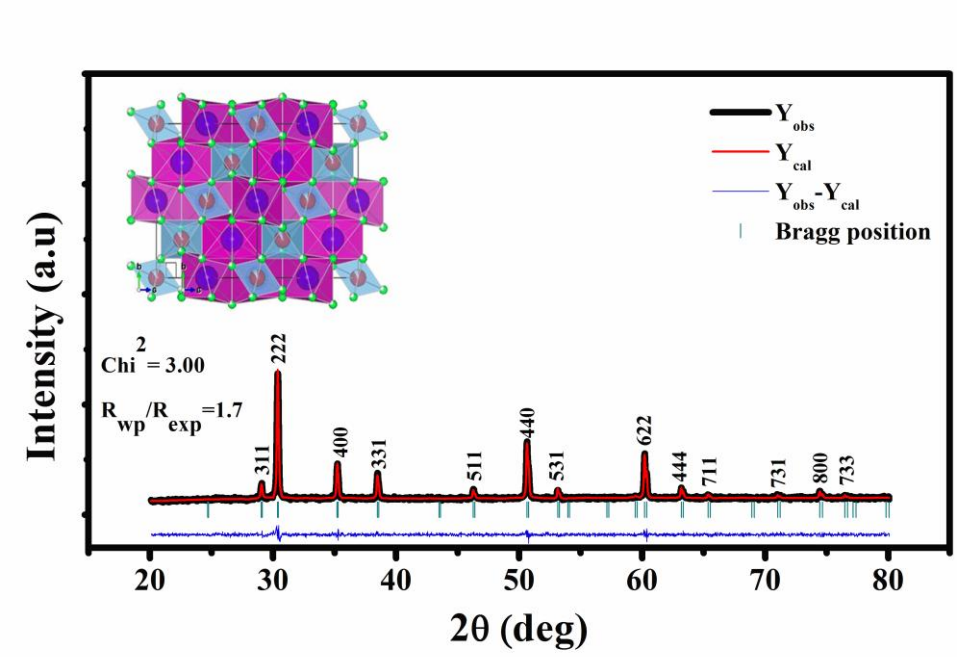

Figure. 3.2: *X-Ray diffraction pattern with Rietveld refinement for $Eu_2Ti_2O_7$. The inset is showing the structure of pyrochlore $Eu_2Ti_2O_7$. Here the blue, red and green spheres representing the position of Eu^{3+}, Ti^{4+} and O^{2-} ions respectively.*

3.3 Results and Discussions

3.3.1 Dc magnetization studies

Dc magnetization measurements of ETO were performed as a function of temperature and field. Fig. 3.3 shows the temperature (T) variation of magnetization (M) following the zero field cooled (ZFC) and field cool (FC) protocols with applied magnetic field of 100 Oe. It shows magnetization (M) increases with decrease in temperature, however, there are few observations: as the temperature decreases from 300K M increases and reaches a maximum at ~90 K. On further decreasing the temperature, a slope change is observed and the system enters in a plateau region in which with temperature very weak variation in magnetization is observed. The plateau region extends down to~20 K and below of which again the slope of the curve changes and a sharp increase in magnetization is observed. The plateau region accounts for the strong crystal field effect (CF) [25]. The sharp increase in M below 10 K may indicate rise of some type of short-range magnetic ordering. However, both the ZFC and FC magnetization curves have the same nature but a small difference is visible between these

two curves, suggesting existence of spin frustration in this system. However, the sharp increase in magnetization at low temperature cannot be attributed to the crystal field effect instead other magnetic interactions, e.g. exchange interactions, dipolar interactions etc., can be possible origin behind such behaviour.

Therefore, to calculate the contributions of these different magnetic properties, high temperature series expansion of the susceptibility $\boldsymbol{(\chi) = C\ [\frac{1}{T} + \frac{\Theta_{cw}}{T^2}]}$ is considered [25,26]. We first plot the $\boldsymbol{\chi T}$ as a function of $\boldsymbol{\frac{1}{T}}$ and then calculate the value of Curie Weiss temperature Θ_{cw}, effective magnetic moment μ_{eff}, exchange interaction energy J_{nn} and dipolar interaction energy D_{nn} from linear fit of the curve (inset (b) of Fig. 3.3). The fit has been done in the temperature range 2-5 K. Here, μ_{eff} is determined from $C= \frac{N\mu_{eff}^2}{3K}$; exchange interaction energy is obtained from $J_{nn} = \frac{3\Theta_{cw}}{zS(S+1)}$, z=6 is the co-ordination number and dipolar interaction energy is determined from $D_{nn}= \frac{\mu_{eff}^2\mu_0}{4\pi r_{nn}^3}$, here r_{nn} is the distance between a Eu^{3+} ion at (000) and its nearest neighbour at (a/4,a/4,0), $\boldsymbol{a}$ being the lattice constant of the unit cell [25,27]. The evaluated values of all the parameters (J_{nn}, D_{nn}, μ_{eff}, Θ_{cw}) obtained from aforementioned formulae have been summarized in Table-3.1. The data for pure $Eu_2Ti_2O_7$ shows nearest neighbour AFM exchange interaction J_{nn} dominates over FM dipole-dipole interaction D_{nn} and Curie-Weiss temperature is small but negative (-1.35 K) which is consistent with the previous report [25].

Isothermal magnetization (M) as a function of magnetic field (H) at 2K (inset of Fig. 3.3) shows the linear behaviour suggesting antiferromagnetic ordering of the system.

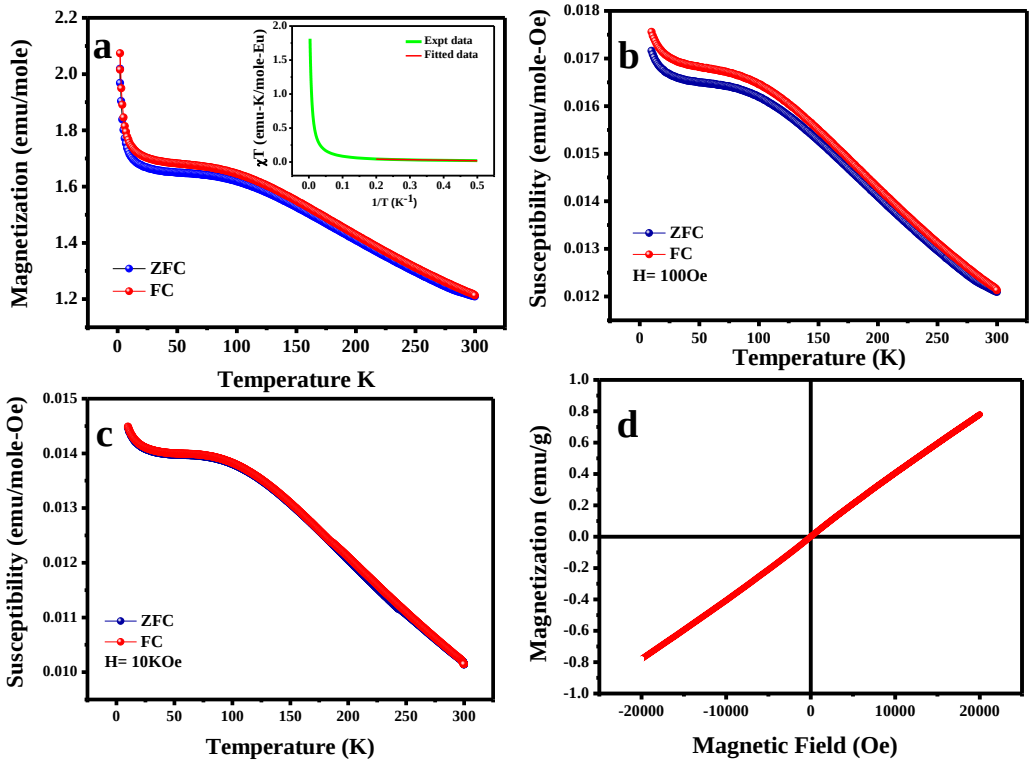

Figure. 3.3: *(a) The temperature variation of magnetization (ZFC and FC) curves at H = 100 Oe for the temperature range of 2–300 K for Eu2Ti2O7. Inset: ''νT vs 1 T '' curve and its linear fit for the range T = 2–5 K. (b): A closer view of ZFC and FC susceptibility curves at 100 Oe showing existence of little thermo-magnetic irreversibility in the data in the temperature range 10–300 K. (c) ZFC and FC susceptibility curves at an increased magnetic field of 10 KOe. (d) The isothermal magnetization curve recorded at 2 K.*

Table-3.1: Showing the magnetic characteristic parameters evaluated from high temperature series expansion of susceptibility study for the temperature range 2 K-5 K.

Sample	Curie-Weiss temperature(Θ_{cw})	Effective magnetic moment (μ_{eff})	Exchange interaction energy (J_{nn})	Dipolar exchange interaction energy (D_{nn})
$Eu_2Ti_2O_7$	-1.35 K	0.679 μ_B	-0.67 K	+0.006 K

3.3.2 Ac magnetization study

To study the spin relaxation process in $Eu_2Ti_2O_7$, ac-susceptibility was performed at the temperature range from 2 K to 80 K at different frequencies. Surprisingly, we observed a frequency dependent transition in the form of a dramatic drop in χ' and the corresponding single peak as expected from Kramers-Kronig relations in χ'' while decreasing temperature below ~35 K [Fig. 3.4 (a and b)], although in the dc susceptibility no prominent transition was observed. The freezing transition observed at such a high temperature is quite unusual and strange, since the structural disorder or the site randomness present in these pyrochlore materials is less than 1%. This directly creates contradiction to the well established spin-glass theory where disorder plays the main role in producing glassy behaviour [28]. However; the strong frequency dependence of these peak positions suggests the existence of a slow magnetic spin relaxation. The freezing temperature $\mathbf{T_f}$ ~35K (for 700 Hz) is obtained from the clear sharp rise in χ'' which is correlated with the sharp drop in χ' [11,19,29]. Below freezing temperature (i.e ~35 K), the dynamic of Eu^{3+} spins response get slowed down as they cannot follow the time varying ac magnetic field, as a consequence, the drop in χ' occurs [20,21]. Therefore, for the present case, the relaxation time of the dynamic spins is longer than the measurement time (which is the inverse of the frequency) such that the system goes to "out of equilibrium" in that time scale, while the energy absorption by the relaxing spins is manifested by the rise of peak in the χ''. In this scenario, it is relevant to mention here that freezing transition was reported earlier in spin ice materials i.e. $Dy_2Ti_2O_7$ and $Ho_2Ti_2O_7$, $Ho_2Sn_2O_7$ etc. at very low temperature (~1 K) [11,12,18,30]. For all these low temperature freezing transitions (~1 K), the thermal energy barrier associated with the spin relaxation is ~20 K. But as mentioned in the introduction that only for the spin ice compound $Dy_2Ti_2O_7$; a further unexpected transition was observed at ~16 K which obeys Debye type exponential relaxation behaviour with thermal energy barrier 210 K. This transition is unusual since it

was not observed in any other spin ice compounds and thus is of particular scientific interest [11,20]. For the last two decades, intense research is going on to investigate the thermally activated transition at 16 K in the frustrated spin ice $Dy_2Ti_2O_7$. However, in our case, we have not observed any low temperature (<4 K) transition but found relatively higher temperature (~34 K, f=700 Hz) spin freezing making the situation much more interesting. To investigate the effect of a dc magnetic field on the spin freezing, we have studied the ac susceptibility with dc bias field of 10 KOe. Fig. 3.4(c & d) shows the graphs for χ' and χ'' as a function of temperature with dc bias H=10 KOe. It is clear from this figure that even after applying such high field, the freezing temperature T_f remains almost unchanged while the drop in χ' decreases a bit and a little suppression occurs in corresponding χ'' peak.

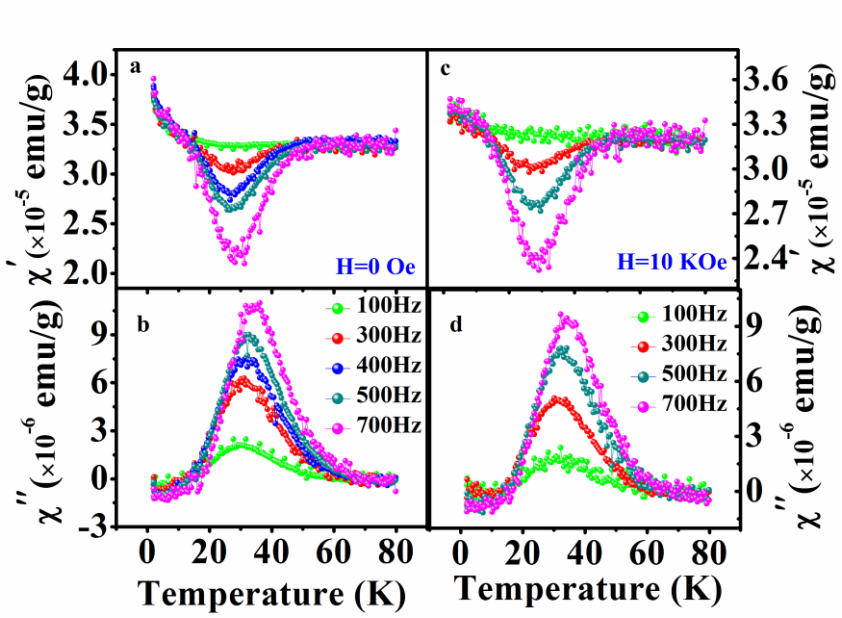

Figure. 3.4: *Temperature variation of ac susceptibility χ' and χ'' at dc fields H=0 Oe (Fig. a & b)and 10KOe for $Eu_2Ti_2O_7$ for different frequencies (Fig. c & d).*

In Fig. 3.5(a & b), we have shown the variation of χ' and χ'' at different dc magnetic fields. Here it is very interesting to note that on application of further higher dc magnetic fields (2 T and 3 T), T_f shows clear shift towards higher temperature and the drop in χ' gets

suppressed (Fig. 3.5(b)). Hence it is in strong contrast with typical spin glass transition. In typical spin glass, the freezing temperature gets shifted towards lower temperature with application of dc magnetic field as the applied field hinders the spins to freeze, but in this case, $\boldsymbol{T_f}$ shifts towards higher temperature which undoubtedly rules out the possibility of spin glass [31]. In spin ice $Dy_2Ti_2O_7$, though similar $\boldsymbol{T_f}$ shift was observed in its 16 K transition but for this case χ' itself got suppressed with dc field, hence qualitatively this transition seems different [12]. However, another way to check whether the present transition is of spin glass type, we have studied freezing temperature $\boldsymbol{T_f}$ as a function of frequency. For a typical spin-glass transition, it is characterized by a parameter $\boldsymbol{p = \frac{\Delta T_f}{T_f \Delta(log f)}}$ [12, 32,33] **,** where the value of $\boldsymbol{p}$ should be of the order of 0.01, where $\boldsymbol{T_f}$ is the freezing temperature at frequency $\boldsymbol{f}$. But in the present investigation, the value we obtained is ~0.286 which is much greater than typical $\boldsymbol{p}$ value for spin glass. Therefore, this result confirms that the observed freezing transition is different from typical spin glass transition. It is though not very surprising because the observed transition is related to lattice geometry and not related to site-disorder which usually gives rise to spin glass behaviour. Again, to further characterize the observed transition, we have fitted the "frequency ($\boldsymbol{f}$) dependence of freezing temperature ($\mathbf{T}_f$)" by Arrhenius law $\boldsymbol{f = f_0 e^{-E_b/K_B T}}$ in the inset of Fig. 3.5(b); where E_b is the thermal energy barrier for spin flipping and f_0 is a measure of the microscopic limiting frequency in the system, K_B being the Boltzman constant [20,21]. The fit shows the thermal energy barrier (E_b) for pure $Eu_2Ti_2O_7$ is 339 K and f_0 is of order MHz which is a reasonable value for spin flipping. The thermal energy barrier (339 K), thus obtained is of the order of the crystal field (CF) energy level spacing between ground state $^7F_0$ and first excited state $^7F_1$ (~378 K or 263 cm^{-1}) [17] which suggests the transition is thermally activated and the energy is of the order of single ion anisotropy energy for Eu^{3+} ions [20,21]. It is pertinent to mention here that the little bifurcation observed between ZFC and FC dc magnetization curves can be attributed to the

geometry driven spin frustration present in the system. The bifurcation becomes more prominent below the freezing temperature suggesting the spin freezing is responsible for enhancing the ZFC-FC bifurcation.

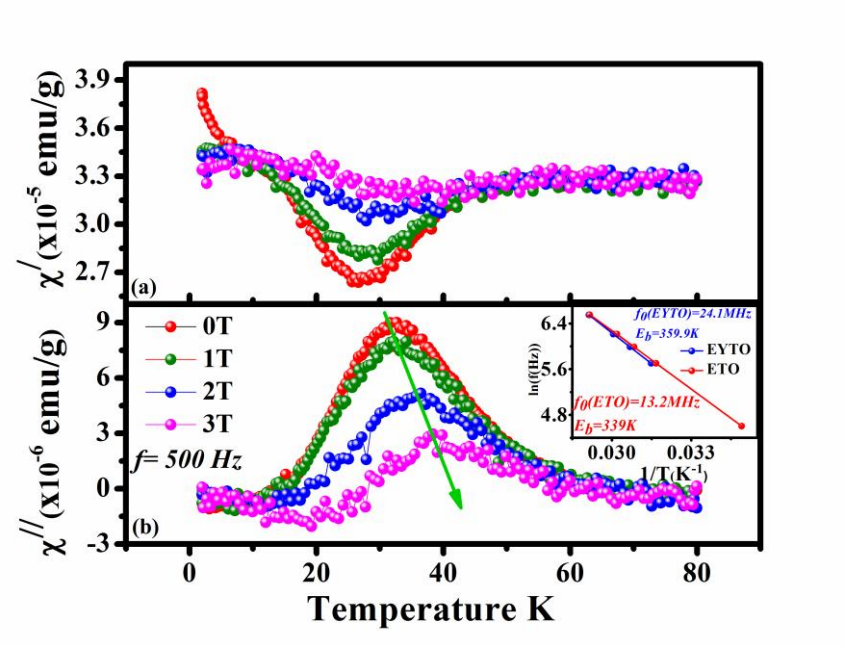

Figure. 3.5: *Temperature dependence of χ' and χ'' at different dc fields at 500Hz. The inset is showing Arrhenius plot for $Eu_2Ti_2O_7$ (ETO) and $EuYTi_2O_7$ (EYTO).*

In order to investigate the underlying freezing mechanism observed in pure $Eu_2Ti_2O_7$, the "frequency dependence of χ''" (Fig. 3.6) have been studied at different temperatures near and below T_f (<36 K). The patterns of the "χ'' curves as a function of frequency f" change in a systematic manner with the temperature approaching towards the freezing temperature T_f. The peaks of the χ'' curves get relatively sharper as it goes near the freezing temperature T_f, suggesting the underlying spin relaxation can presumably be attributed to the individual spin relaxation which is known as single ion freezing [12]. In general, a sharp peak indicates the distribution of spin relaxation times is very narrow around a "single characteristic time τ" which is defined as $\tau=1/f$, where $\chi''(f)$ having its maximum at f [12,20,29]. In contrast, in conventional spin-glass systems, the $\chi''(f)$ shows a broad feature thus suggesting a spreading

of relaxation times over several decades [12]. Thus the observed spin freezing is qualitatively different from spin-glass freezing. However, it is noteworthy to mention here that the sharpness of the $\chi''(f)$ curves decreases a little bit as temperature cools below the freezing temperature T_f but still remains in a limit to show single spin relaxation process. Another way to characterize the observed spin freezing process is to fit the "χ'' (normalized to its maximum value) *vs.* the normalized frequency $\frac{f}{f_{peak}}$ " curves (top inset of Fig. 3.6) by ***Casimir-du Pŕe*** relation which is typically used as to predict a single ion relaxation process [12,20]. The relation is $\chi''(f) = f\tau[(\chi_T - \chi_S)/(1 + f^2\tau^2)]$, where χ_T is isothermal susceptibility in the limit of low frequency and χ_S is the adiabatic susceptibility in the limit of high frequency. It is observed that our experimentally obtained curves below and near T_f (27.16 K and 33.16 K), are relatively narrower than the theoretically fitted data, suggesting the observed spin freezing is caused by individual spin relaxation process. Further, for a single spin relaxation mode, it is theoretically predicted that Cole-Cole (Argand) plot of "χ'' as a function of χ'", should show a semicircular nature [12]. In (bottom) inset of Fig. 3.6, the Cole- Cole plots have been shown at different temperatures (below and near T_f). Interestingly, the curves clearly trace the semicircular path thus indicating the presence of the single spin relaxation process in the observed spin freezing. The change in the peak positions of χ'', implies slight change in the relaxation times as temperature decreases.

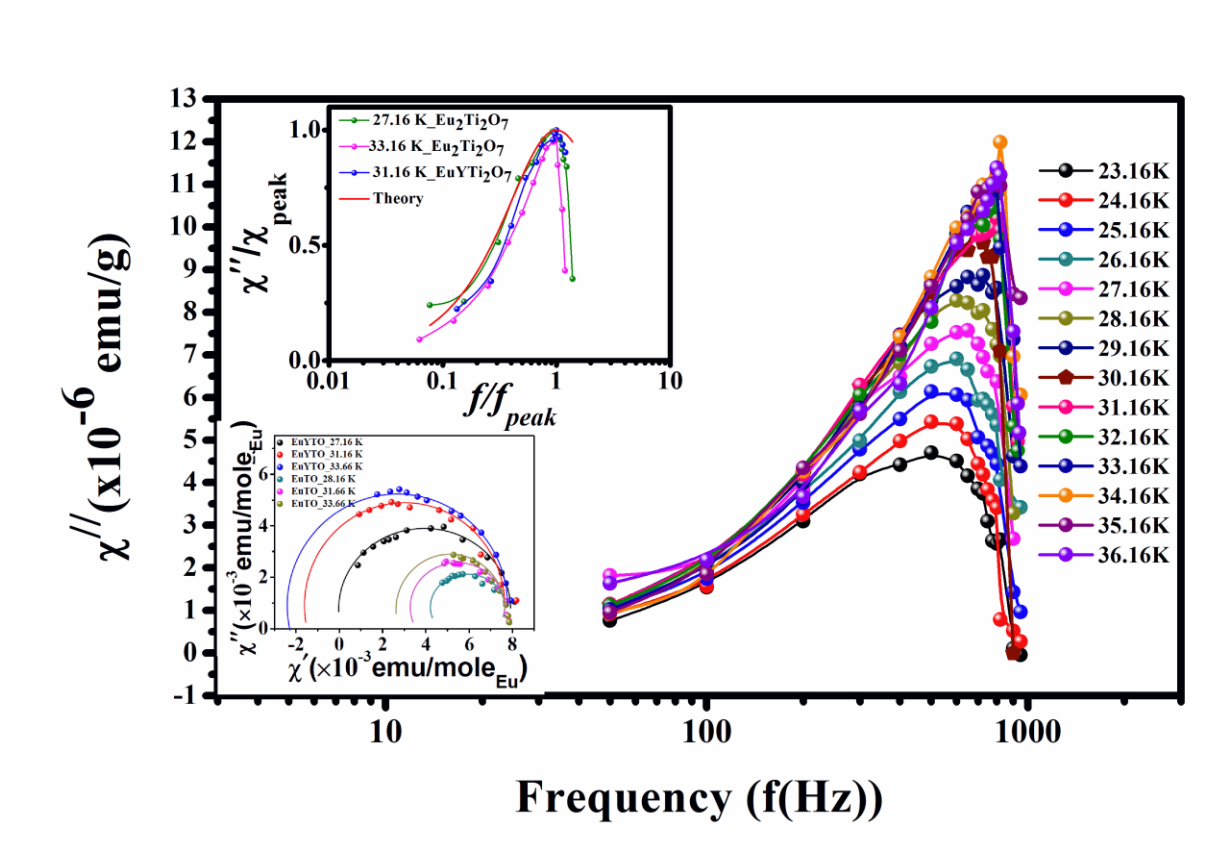

Figure. 3.6: *Frequency dependence of χ'' at different temperatures for pure $Eu_2Ti_2O_7$. Inset(top) showing the normalized χ'' as a function of f/f_{peak} and its theoretical fitting by Casimir du pŕe relations at different temperatures for pure and nonmagnetic diluted samples. Inset (bottom) showing Cole Cole (Argand) plot of "χ'' Vs χ'" at different temperatures for pure and diluted samples.*

In the present scenario, to confirm the nature of this spin freezing transition, we investigated the effect of non-magnetic dilution in our system. We have replaced 50% of Eu^{3+} ions by non-magnetic Y^{3+} ions to change the local environment of Eu ions such that in each of the corner shared tetrahedra there are two Eu ions and two Y ions effectively. Hence, this non-magnetic dilution causes increase in effective distance between Eu ions thus lowering the local Eu-Eu spin correlations. It is obvious that if the observed spin freezing (T<35 K) requires spin-spin correlation, then the non-magnetic dilution should suppress the spin

freezing. Interestingly, in the ac susceptibility (Fig. 3.7) of non-magnetic diluted sample $EuYTi_2O_7$ (EYTO), the spin freezing transition is observed to become more pronounced instead of being diminished. This observation confirms the single ion nature of the observed spin freezing, where local spin-spin correlation is not required at all [21]. The possible explanation for the enhancement of the spin freezing with non-magnetic dilution can be given on the basis of the change in the local environment of the participating Eu^{3+} spins. In Fig. 3.7(c), the increased drop in χ' indicates a further increase in the characteristic relaxation time of spin flipping with Y^{3+} substitution i.e. the spins take longer time to relax. From, top inset of Fig. 3.6, it is clear that even after 50% dilution, the χ'' (f) remains narrow enough to support single ion freezing. The calculation of thermal energy barrier (E_b) by Arrhenius plot for EYTO gives a value ~360 K which is greater than that of ETO (339 K) [inset of Fig. 3.5(b)]. The increased E_b causes more delay in the spin relaxation, thus enhancing the spin freezing with dilution. The small increase in thermal energy barrier E_b is seemingly caused by slight alteration of lattice constant and electronic structures of the system [21]. Bottom inset of Fig. 3.6, shows even after 50% non-magnetic dilution, the Cole-Cole plot follows closely semicircular path, suggesting persistence of single ion process. Therefore, the observed transition is fundamentally a single ion process and is not affected by spin-spin correlation. Additionally, we have also performed the ac susceptibility measurements for pure $Y_2Ti_2O_7$ (YTO) which are shown in Fig. 3.7(e and f) at a frequency of 500 Hz. No spin freezing transition was observed for pure YTO which was expected as Y^{3+} ions are non-magnetic in nature. This again confirms the observed spin freezing to be associated purely to the Eu^{3+} spins. However, a noticeable difference between spin freezing (16 K) observed in $Dy_2Ti_2O_7$ (DTO) and the spin freezing observed in ETO is that for DTO freezing temperature (T_f) increases with dilution but for ETO, upto 50% dilution, it remains almost unchanged (Fig. 6(d)). However, it deserves further study to fully understand the underlying physics.

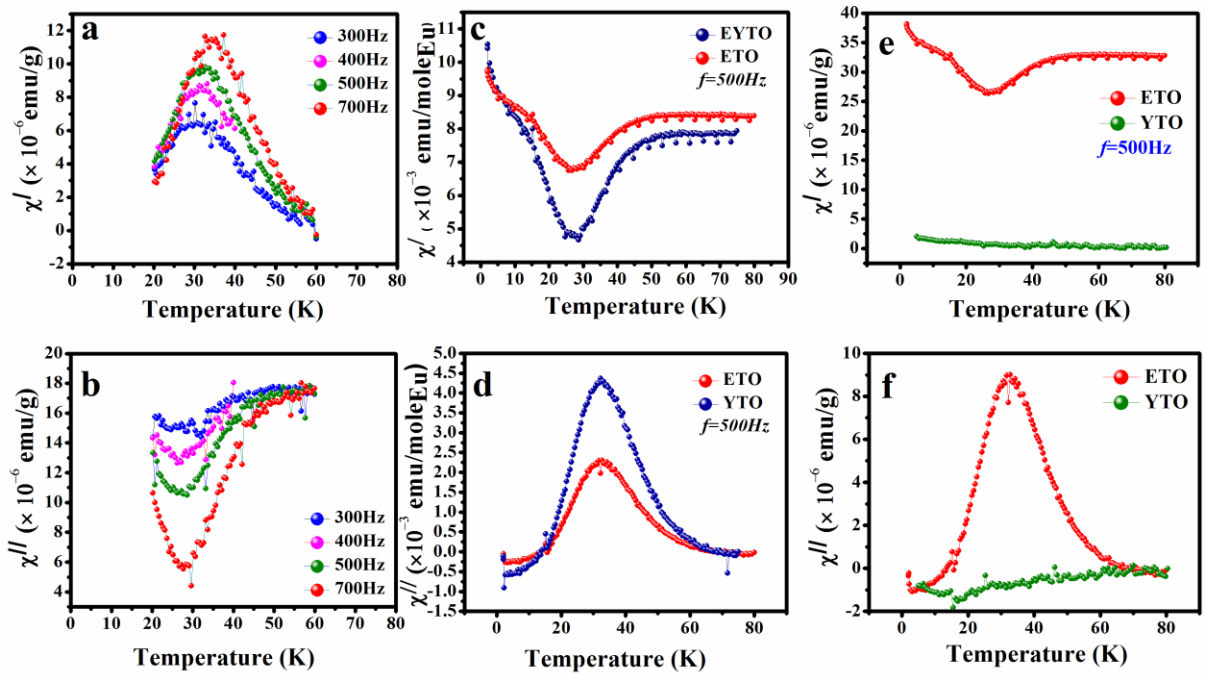

Figure. 3.7: *(a & b) showing temperature variation of ac susceptibility χ' and χ'' for diluted sample EYTO. Fig. (c and d) show comparison of temperature dependence of χ' and χ'' for pure and diluted samples at 500Hz. Fig. e and f showing the temperature variation of χ' and χ'' at 500Hz for pure ETO and YTO.*

3.4 Conclusion

In summary, ac susceptibility study has revealed a sharp spin freezing in pyrochlore ETO below T_f~35 K. Analysis yielded the transition to be a thermally activated phenomenon and the thermal energy barrier (E_b ~339 K) as extracted from the frequency dependence of ac χ'' peak positions, is found to be of the order of single ion anisotropy energy i.e the energy level spacing of CF levels. The spin freezing transition is found to be fundamentally different from conventional spin glass transitions. In common spin glass materials, the presence of large scale structural and chemical disorders cause the random freezing of spins, where the spins

are almost isotropic in nature. In contrast, for pyrochlore ETO, the observed freezing is driven by local geometrical spin frustration where the spins have anisotropy (SIA) which offers them less freedom for movement. Analysis by Cole-Cole plot and Casimir-du Pŕe relation suggested the single ion relaxation process to be involved in the observed spin freezing. Further analysis by non-magnetic dilution with Y^{3+} ions, confirmed the single ion freezing process by ruling out the probability of need for "local spin-spin correlation" in the spin freezing process. More interestingly, to date the observed spin freezing temperature ~35 K is the highest freezing temperature as the earlier reported spin freezing was at ~16 K in DTO. Thus, the observed spin freezing transition is significantly unusual by its nature and further investigations may explore the understanding of spin dynamics in such site-ordered geometrically frustrated systems. Other theoretical models or neutron experiments may help to confirm its origin further.

References

1. J. S. Gardner, M. J. P. Gingras and J. E. Greedan, Rev. Mod. Phys. **82** (2010) 53
2. C. Castelnovo, R. Moessner and S. L. Sondhi, Nature **451** (2008) 42
3. S. T. Bramwell, M. J. P. Gingras, Science **294** (2001) 1495
4. L. Balents , Nature **464** (2010) 199
5. T. Taniguchi, H. Kadowaki, H. Takatsu, B. Fak, J. Ollivier, T. Yamazaki, T. J. Sato, H. Yoshizawa , Y. Shimura and T. Sakakibara et. al. Phys. Rev. B **87** (2013) 060408
6. J. S. Gardner, A. Keren, G. Ehlers, C. Stock, E. Segal, J. M. Roper, B. Fak, M. B. Stone, P. R. Hammar, and D. H. Reich et. al.; Phys. Rev. B **68** (2013) 180401(R)
7. G. Ehlers, J.E. Greedan, J R Stewart, K C Rule, P Fouquet, A L Cornelius, C Adriano , G Pagliuso, Y. Qiu and J. S. Gardner Phys. Rev. B **81** (2010) 224405
8. D. K. Singh, Y. S. Lee, Phys. Rev. Lett. **109** (2012) 247201
9. S. Iguchi, Y. Kumano, K. Ueda, S. Kumakura and Y. Tokura, Phys. Rev. B **84** (2011) 174416
10. A. P. Ramirez, A. Hayashi, R. J. Cava, R. Siddharthan and B. S. Shastry, Nature **399** (1999) 333
11. J. Snyder, B.G. Ueland , J. S. Slusky, H. Karunadasa, R. J. Cava, and P. Schiffer, Phys. Rev. B **69** (2004) 064414
12. J. Snyder, J.S. Slusky, R. J. Cava, and P. Schiffer, Nature **413** (2001) 48
13. J. Oitmaa, R. R. P. Singh , B. Javanparast, A. G. R. Day, B. V. Bagheri, and M. J. P. Gingras ,Phys Rev B **88** (2013) 220404
14. L. Savary, K. A. Ross, B. D. Gaulin, J. P. C. Ruff and L. Balents, Phys Rev Lett, **109**(2012)1672201

15. J. D. M. Champion, M. J. Haris, P. C. W. Holdsworth, A. S. Wills, G. Balakrishnan, S. T. Bramwell, E. Cizmar, T. Fennell, J. S. Gardner and J. Lago et. al., Phys. Rev. B **68** (2003) 020401(R)

16. H. W. J. Blote, R. F. Weilinga, W. J. Huiskamp, Physica **43** (1969) 549

17. A. Nag (Chattopadhyay), P. Dasgupta, Y. M. Jana, D. Ghosh; J. Ally. Comp **384** (2004) 6

18. K. Matsuhira, Y. Hinatsu, K. Tenya and T. Sakakibara, J. Phys. : Cond. Matt. **12** (2000) L-649

19. G. Ehlers, A. L. Cornelius , M. Orendac, M. Kajnakova, T. Fennell, S. T. Bramwell and J. S. Gardner, J. Phys. : Cond. Matt. **15** (2003) L-9

20. J. Snyder, J. S. Slusky, R. J. Cava, and P. Schiffer, Phys. Rev. B **66** (2002) 064432

21. J. Snyder, B. G. Ueland, A. Mizel, J. S. Slusky, H. Karunadasa, R. J. Cava and P. Schiffer, Phys. Rev. B **70** (2004) 184431

22. X. Ke, D.V. West, R. J. Cava and P. Schiffer, Phys. Rev. B **80** (2009) 144426

23. H. Xing, M. He, C. Feng, H. Guo, H. Zeng and Z. Xu, Phys. Rev. B **81** (2010) 134426

24. L. D. C. Jaubert, P. C. Holdsworth, Nat. Phys.**5**, (2009) 258

25. P. Dasgupta, Y. M. Jana, A. N. Chattopadhyay, R. Higashinaka, Y. Maeno and D Ghosh, J. Phys. Chem. Solid. **68** (2007)347

26. M. J. P. Gingras , B. C. den Hertog, M. Faucher, J. S. Gardner, S. R. Dunsiger, L. J. Chang, B. D. Gaulin, N. P. Raju and J. E. Greedan, Phys. Rev. B **62** (2000) 6497

27. N.P. Raju, M. Dion, M. J. P. Gingras , T. E. Mason, J. E. Greedan, Phys. Rev. B **59** (1999) 14489

28. S. T. Bramwell, M. J. Harris, J. Phys. : Cond. Matt. **10** (1998) L215

29. J. Snyder, B. G. Ueland, J. S. Slusky, H. Karunadasa, R. J. Cava, Ari Mizel, and P.

Schiffer, Phys. Rev. Lett. **91**(2003)107201

30. G. Ehlers, A. L. Cornelius, T. Fennel, M. Koza, S.T. Bramwell and J. S. Gardner, J.Phys.: Cond. Matt **16**(2004) S635
31. K. Manna, A. K. Bera, M. Jain, S. Elizabeth, S. M. Yusuf and P. S. Anil Kumar, Phys. Rev B **91**, (2015) 224420
32. M. L. Dalberg, M. J. Matthews, P. Jiramongkolchai, R. J. Cava, and P. Schiffer, Phys. Rev. B **83** (2011)140410(R)
33. S. Ghara, B. G. Jeon, K. Yoo, K. H. Kim, and A. Sundaresan, Phys. Rev B **90** (2014) 024413